

## Electronic Supplementary Information

### **Inter-phase charge and energy transfer in Ruddlesden–Popper 2D perovskites: critical role of the spacing cations**

Kaibo Zheng,<sup>\*af</sup> Yani Chen,<sup>b</sup> Yong Sun,<sup>b</sup> Junsheng Chen,<sup>a</sup> Pavel Chábera,<sup>a</sup> Richard Schaller,<sup>c</sup>  
Mohammed J. Al-Marri,<sup>e</sup> Sophie E Canton,<sup>de</sup> Ziqi Liang<sup>\*b</sup> and Tõnu Pullerits<sup>\*a</sup>

<sup>a</sup>Department of Chemical Physics and NanoLund, Lund University, Box 124, 22100, Lund, Sweden

<sup>b</sup>Department of Materials Science, Fudan University, Shanghai 200433, China

<sup>c</sup>Center for Nanoscale Materials, Argonne National Laboratory, 9700 Cass Avenue, Argonne, Illinois 60439, United States

<sup>d</sup>ELI-ALPS, ELI-HU Non-Profit Ltd., Dugonicster 13, Szeged 6720, Hungary

<sup>e</sup>Attoscience Group, Deutsche Elektronen Synchrotron (DESY), Notkestrasse 85, D-22607 Hamburg, Germany

<sup>f</sup>Gas Processing Center, College of Engineering, Qatar University, PO Box 2713, Doha, Qatar

#### AUTHOR INFORMATION

#### **Corresponding Author**

\*Email: [kaibo.zheng@chemphys.lu.se](mailto:kaibo.zheng@chemphys.lu.se) (K.Z.)

\*Email: [zqliang@fudan.edu.cn](mailto:zqliang@fudan.edu.cn) (Z.L.)

\*Email: [tonu.Pullerits@chemphys.lu.se](mailto:tonu.Pullerits@chemphys.lu.se) (T.P.)

## Experimental Section

**Materials.** All chemicals were purchased from J&K Scientific, Ltd. (China) and used as received.  $\text{PbI}_2$  and  $\text{CH}_3\text{NH}_3\text{I}$  were purchased from Maituowei Ltd. (China).

**Fabrication of 2D perovskite films.** n-BA perovskites and iso-BA perovskites were prepared according to our previous report.<sup>[1]</sup> The precursor solutions (40 wt%) were made by mixing  $\text{PbI}_2$ , HI,  $\text{CH}_3\text{NH}_3\text{I}$ , and n- $\text{C}_4\text{H}_9\text{NH}_2$  (or iso- $\text{C}_4\text{H}_9\text{NH}_2$ ) at a stoichiometric ratio of 4:2:3:2 in DMF, followed by stirring for 30 min in a nitrogen-filled glovebox. Then the solution was filtered through a 0.45  $\mu\text{m}$  nylon filter before use.  $(\text{n-BA})_2(\text{MA})_3\text{Pb}_4\text{I}_{13}$  and  $(\text{iso-BA})_2(\text{MA})_3\text{Pb}_4\text{I}_{13}$  films were obtained by spin-coating their precursor solutions at 5000 rpm for 60 s at room temperature on quartz substrate for further measurements.

**Characterization.** X-ray diffraction (XRD) pattern data for  $2\theta$  values were collected with a Bruker AX D8 Advance diffractometer with nickel filtered Cu  $K\alpha$  radiation ( $\lambda = 1.5406 \text{ \AA}$ ). Ground-state absorption spectra were measured in a UV–Vis absorption spectrophotometer (PerkinElmer, Lambda 1050) equipped with integrating sphere to exclude signal due to light scattering. Steady-state photoluminescence was measured using a FluoroMax@-4 spectrofluorometer (HORIBA JOBIN YVON, Inc., Edison, NJ) with the excitation beam at 500 nm. The PL intensity was then corrected by absorbed photon numbers at the exciting light wavelength. Transient absorption (TA) experiments were performed by using a femtosecond pump-probe setup in nitrogen atmosphere. Laser pulses (800 nm, 80 fs pulse length, 1 kHz repetition rate) were generated by a regenerative amplifier (Spitfire XP Pro) seeded by a femtosecond oscillator (Mai Tai SP, both Spectra Physics). The pump pulses at 400 nm were generated by a BBO crystal as a second harmonic of the laser. The used excitation photon fluxes are  $3 \times 10^{12}$  and  $1.5 \times 10^{14}$  photons/ $\text{cm}^2$ /pulse. For the probe, we used the super-continuum

generation from a thin CaF<sub>2</sub> plate. The mutual polarization between pump and probe beams was set to the magic angle (54.7°) by placing a Berek compensator in the pump beam. The probe pulse and the reference pulse were dispersed in a spectrograph and detected by a diode array (Pascher Instruments). In order to avoid photo-damage, the sample was moved to a fresh spot after each time delay point. Global SVD analysis was performed with the Glotaran software package (<http://glotaran.org>). These methods yield more accurate fits of rate constants because they treat the full data set as a whole. A simple sequential decay model with various components is chosen for every fitting. Time-resolved photoluminescence (TRPL) spectra were obtained using a streak camera (Hamamatsu, C6860). The laser source is an amplified titanium/sapphire laser providing 800 nm 35-fs pulses at 2 kHz which is then frequency doubled for 400 nm excitation. The absolute PL quantum yield (PLQY) was measured by using a standard spectrometer with integrating sphere (Horiba) using the same fs pulse laser as in TA and TRPL measurement.

## Results and Discussion

**Calculation of the photon density.** The photon density  $n_0$  in 2D perovskites can be calculated by:  $n_0 = \sigma N$  where  $N$  is the excitation fluence  $3 \times 10^{12}$  ph/cm<sup>2</sup>/pulse, and  $\sigma$  is absorption cross section of n-BA perovskite films. It can be extracted from the absorbance  $A$  from the absorption spectra:  $A = \sigma d$  where  $d$  is the thickness of the film. Here, we obtained an  $A$  value of 0.28 at 400 nm wavelength for a 285 nm thick film as shown in the cross-section view of the SEM image (Fig. S1) which gives a  $\sigma$  value of  $1 \times 10^4$  cm<sup>-1</sup>.

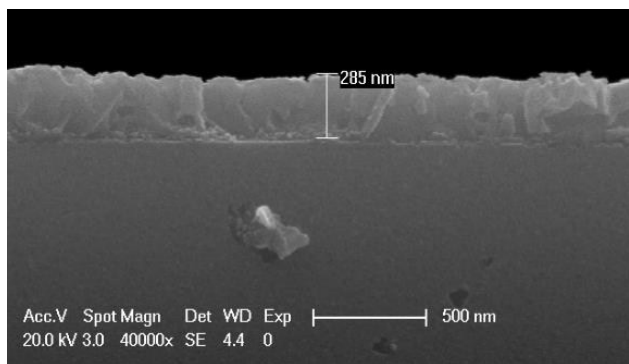


**Fig. S1** SEM image of as-obtained n-BA perovskite film.

**Spatially dependent TA measurements of the 2D perovskites.** When we performed TA measurements, the position of the overlapping pump and probe beams is changed for every scan by  $300\ \mu\text{m}$  (with the beam size of  $100\ \mu\text{m}$ ). We compared the TA spectra of each scan and found that the differences are negligible. As shown in the Fig. S2, the initial TA spectra at 1 ps and the TA kinetics at 640 nm for 4 different spots are basically the same. These results mean that in tens of micrometer scale the film is a homogeneous mixture of the 2D phases.

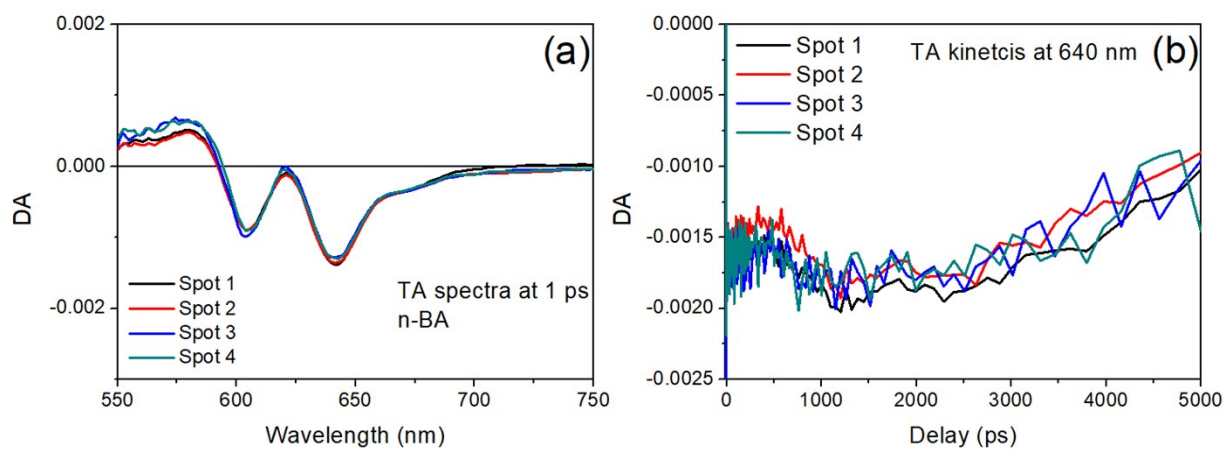


**Fig. S2** TA spectra and kinetics measured at different spots of the samples with spatial variation of  $300\ \mu\text{m}$ .

**Calculation of the initial fraction of free charges and excitons after photoexcitation.** The equilibrium ratio between the free charges and excitons after photoexcitation can be calculated by

using the Saha–Langmuir equation which has been widely used for perovskite systems.<sup>2</sup> According to the Saha-Langmuir theory the fraction of free charges over the total density of excitation,  $x$ , can be expressed as:

$$\frac{x^2}{1-x} = \frac{1}{n} \left( \frac{2\pi\mu k_B T}{h^2} \right)^{1.5} e^{-\frac{E_b}{k_B T}}$$

We take the average exciton binding energy ( $E_b$ ) of 175 meV,<sup>3</sup> use the effective exciton mass  $\mu = 0.2 m_0$  in 2D perovskites reported by other groups.<sup>4</sup> The excitation density  $n$  is calculated from the photon flux  $f$  in photons/cm<sup>2</sup> multiplied by absorption coefficient  $\epsilon$ :  $n = f\epsilon$ , where  $\epsilon$  for n-BA and iso-BA were estimated to be around 1E4 cm<sup>-1</sup> as discussed above. We obtain the fraction of free charges 60 % at lowest excitation fluence of 3E12 ph/cm<sup>2</sup>. At the highest excitation fluence of 1E14 ph/cm<sup>2</sup>, however, the fraction of free carrier would only be 2%.

### Spectral feature of free carriers and excitons in TA spectrogram.

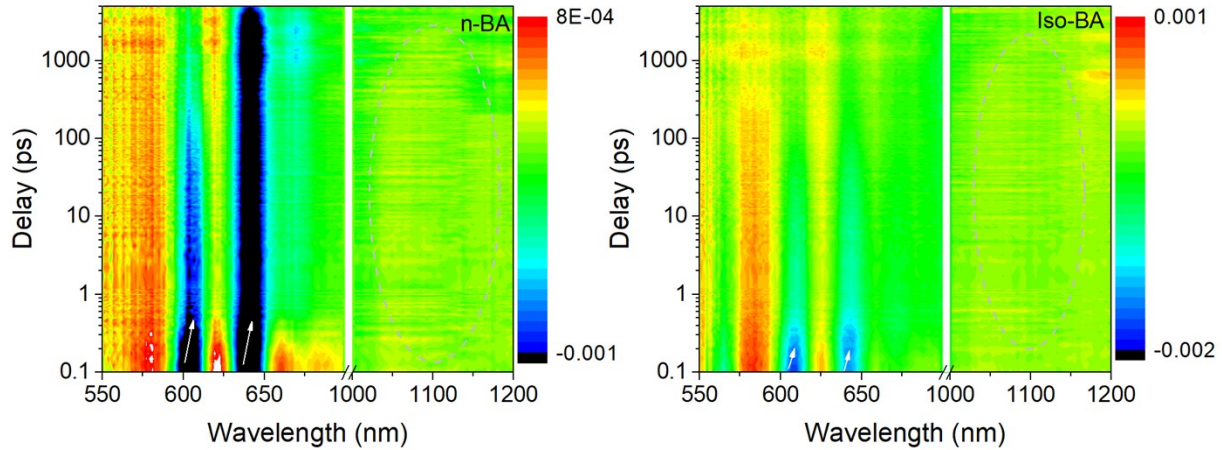


**Fig. S3** TA spectrogram of n-BA and iso-BA excited at 3E12 ph/cm<sup>2</sup> with extended probe window to 1200 nm. The white arrows show the blue-shift of exciton resonance, the dashed gray oval at IR region indicates the signal from the photo-generated free carriers.

**TA kinetics and corresponding SVD fitting.** Fig. S4 shows the TA kinetics with fitted curves from SVD analysis at the bleach positions of each phase in two samples at low excitation

condition. The grey area at the early time scale indicates the co-existence of depopulation of excited states at small- $n$  phases and population of excited states at large- $n$  phases.

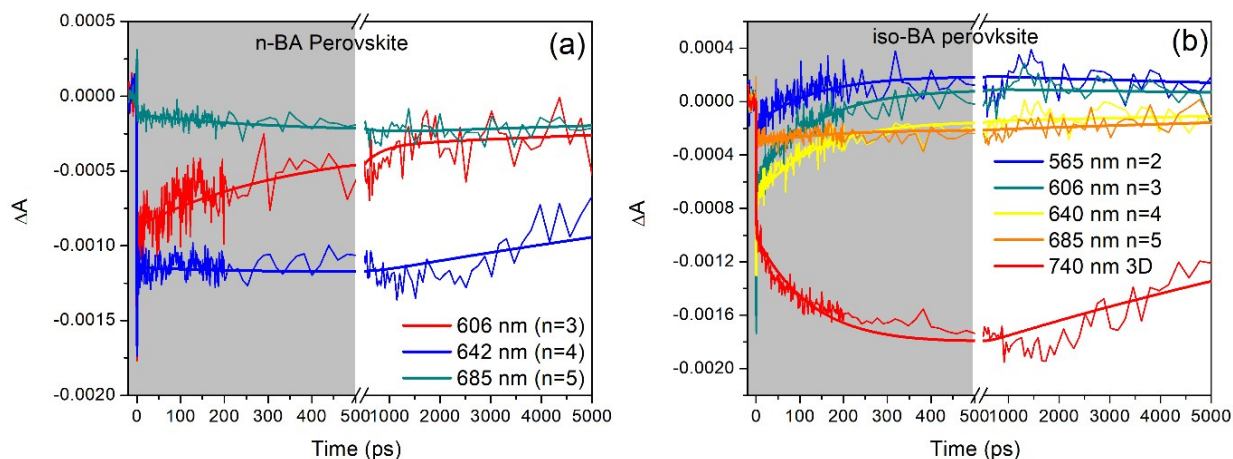


**Fig. S4** TA kinetics (thin lines) at the bleach minima of each phases with the SVD fitting curves (thick lines) for n-BA and iso-BA perovskites corresponding to Fig. 2 in the main text.

**Luminescence quantum yield.** Fig. S5 displays the absolute PLQY of iso-BA and n-BA 2D perovskites with excitation fluence changing from  $1E11$  to  $1E13$   $\text{ph}/\text{cm}^2$ . The PLQY first increases with the excitation intensity increase which is due to the state filling of the long-lived trap states. Afterwards it starts to decline due to the high-order nonradiative Auger recombination.

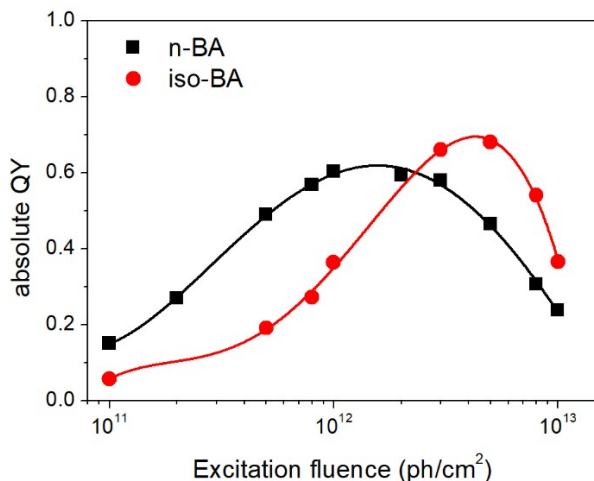


**Fig. S5** Absolute PLQY for n-BA and iso-BA measured with fs laser pulses at 400 nm with various excitation fluence comparable to TA and TRPL measurement.

**Effect of hot casting on the TA dynamics.** Fig. S6 shows the TA spectra and the corresponding SVD fitting of an n-BA perovskite film prepared by hot casting method. The similar charge transfer component with lifetime of 300 ps (red line in Fig. S4b) to RT prepared sample can be observed indicating the orientation of the 2D plane does not affect the inter-phase charge transfer dynamics.

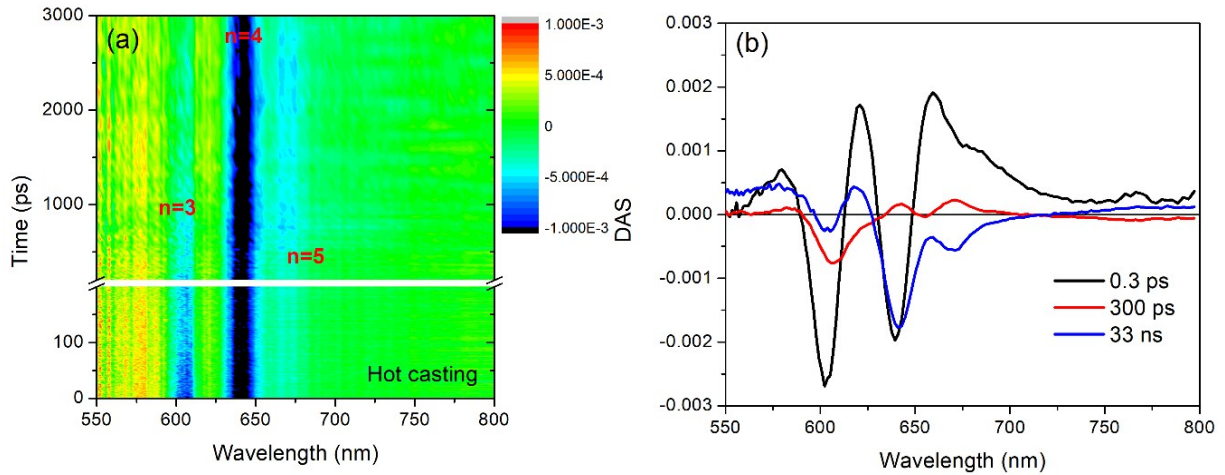


**Fig. S6** (a) TA spectra of n-BA perovskite film prepared using hot-casting method with 400 nm excitation at laser fluence of  $3 \times 10^{12}$  ph/cm<sup>2</sup>/pulse, and (b) SVD fitted spectral components of the corresponding TA spectra.

**$\Delta A$ ,  $\Delta A^{-1}$ ,  $\Delta A^{-2}$  vs time plot in TA spectra.** Fig. S7 plots the  $\Delta A$ ,  $\Delta A^{-1}$ , and  $\Delta A^{-2}$  vs time from TA kinetics of n-BA samples at high excitation condition. The best linear relationship for  $\Delta A^{-2}$  vs time suggests that the third-order recombination dominates the charge carrier decay in all 2D phases in n-BA. For iso-BA sample, the early time delay complies well with the first-order recombination instead, as shown in Fig. S8.

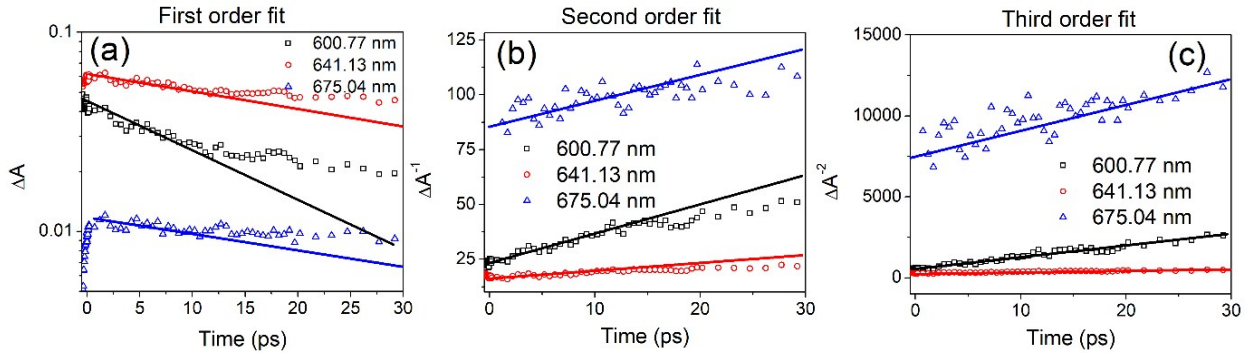


**Fig. S7** (a)  $\Delta A$ , (b)  $\Delta A^{-1}$ , and (c)  $\Delta A^{-2}$  vs time plot extracted from the TA kinetics at the bleaches of each 2D phases of 600 nm, 641 nm and 675 ns from n-BA perovskite film excited at high excitation intensity ( $1.5 \times 10^{14}$  ph/cm<sup>2</sup>/pulse).

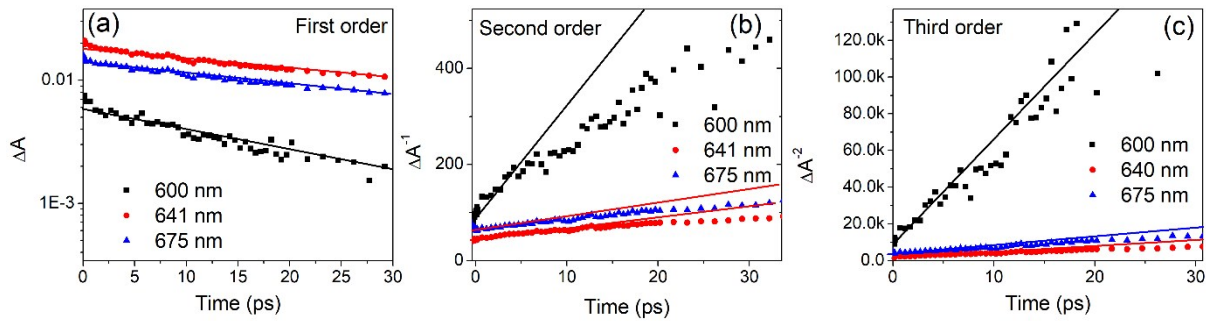


**Fig. S8** (a)  $\Delta A$ , (b)  $\Delta A^{-1}$ , and (c)  $\Delta A^{-2}$  vs time plot extracted from the TA kinetics at the bleaches of each 2D phases of 600, 641 and 675 nm from iso-BA perovskite film excited at high excitation intensity ( $1.5 \times 10^{14}$  ph/cm<sup>2</sup>/pulse)

**Excitation intensity dependent TA measurement.** Fig. S9 shows the TA spectrograms of n-BA and iso-BA perovskite with excitation fluence changing from  $3E12$  to  $1E14$  ph/cm<sup>2</sup>. A general excited state lifetime shortening can be observed by the changes of the bleach decay as indicated by red arrows. In n-BA sample, only at lowest excitation intensity, the inter-phase charge transfer can be observed as the concurrent decay of bleach at small n phase with rise of bleach at large n phase as indicated by the grey arrow. However, in iso-BA such excited state population transfer always exists even at the higher excitation intensities. This clearly confirms our argument

that in iso-BA sample, the inter-phase charge transfer will not be surpassed by the fast Auger charge recombination.

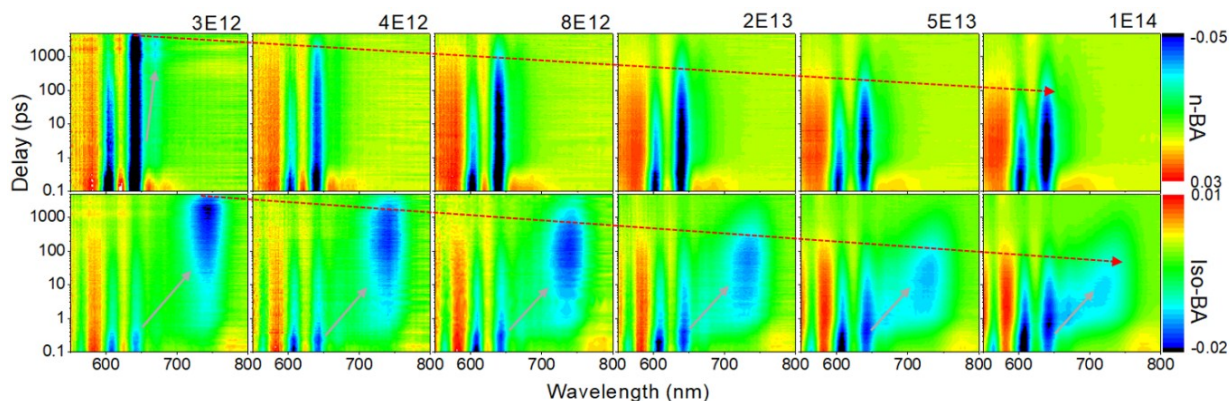


**Fig. S9** TA spectrogram of n-BA and iso-BA perovskites with excitation fluence from 3E12 ph/cm<sup>2</sup> to 1E14 ph/cm<sup>2</sup>, the red arrows indicate the speeding up of the ground state bleach while the grey arrows indicate the inter-phase charge transfer.

## References

1. Y. Chen, Y. Sun, J. Peng, W. Zhang, X. Su, K. Zheng, T. Pullerits and Z. Liang, *Adv. Energy Mater.*, 2017, **7**, 1700162.
2. V. D'Innocenzo, G. Grancini, M. J. Alcocer, A. R. Kandada, S. D. Stranks, M. M. Lee, G. Lanzani, H. J. Snaith and A. Petrozza, *Nat. Commun.*, 2014, **5**, 3586.
3. J.-C. Blancon, H. Tsai, W. Nie, C. C. Stoumpos, L. Pedesseau, C. Katan, M. Kepenekian, C. M. M. Soe, K. Appavoo, M. Y. Sfeir, S. Tretiak, P. M. Ajayan, M. G. Kanatzidis, J. Even, J. J. Crochet and A. D. Mohite, *Science*, 2017, **355**, 1288–1292.
4. J.-C. Blancon, A. V. Stier, H. Tsai, W. Nie, C. C. Stoumpos, B. Traoré, L. Pedesseau, M. Kepenekian, S. Tretiak, S. A. Crooker, C. Katan, M. G. Kanatzidis, J. J. Crochet, J. Even, A. D. Mohite, arXiv:1710.07653.